Augmented fluid-structure interaction systems for viscoelastic pipelines and blood vessels

Giulia Bertaglia *

* Department of Mathematics and Computer Science
University of Ferrara
Ferrara, Italy
e-mail: giulia.bertaglia@unife.it

Key words: fluid–structure interaction, compliant ducts, viscoelastic effects, finite volume methods, IMEX Runge–Kutta schemes

Abstract: *In this work, innovative 1D hyperbolic models able to predict the behavior of the fluid-structure interaction mechanism that underlies the dynamics of flows in different compliant ducts are presented. Starting from the study of plastic water pipelines, the proposed tool is then applied to the biomathematical field to reproduce the mechanics of blood flow in both arteries and veins. With this aim, various different viscoelastic models have been applied and extended to obtain augmented fluid-structure interaction systems in which the constitutive equation of the material is directly embedded into the system as partial differential equation. These systems are solved recurring to Finite Volume Methods that take into account the recent evolution in the computational literature of hyperbolic balance laws systems. To avoid the loss of accuracy in the stiff regimes of the proposed systems, asymptotic-preserving Implicit-Explicit Runge-Kutta schemes are considered for the time discretization, which are able to maintain the consistency and the accuracy in the diffusive limit, without restrictions due to the scaling parameters.*

1 INTRODUCTION

Mathematical models and numerical methods are a powerful resource for better understanding phenomena and processes throughout the fluid dynamics field, allowing significant reduction in the costs, which would otherwise be required to perform laboratory experiments, and even allowing to obtain useful data that could not be gathered through measurements.

The correct characterization of the interactions that occur between the fluid and the wall that surrounds it is a fundamental aspect in all contexts involving deformable ducts, which requires the utmost attention at every stage of both the development of the computational method and the interpretation of the results and their application to cases of practical interest. Concerning flexible plastic pipes, which are playing an increasingly important role in hydraulic systems due to their cost-effectiveness and ease of installation, it has been demonstrated that the choice to characterize the fluid-structure interaction (FSI) behavior through a simple elastic law leads to consistent errors in the predictions of the pressure trends when studying hydraulic transients phenomena [7]. In fact, almost without exceptions, polymers manifest a viscoelastic behavior, responding to external forces in an intermediate way between the behavior of an elastic solid and a viscous liquid [19], and the adoption of a proper viscoelastic constitutive law for the definition of the FSI mechanism results fundamental [11].

Viscoelasticity is characterized by 3 primary features [14]:

1. *Creep*, which describes a material in continuous deformation over time when it is maintained under constant stress;

2. *Stress relaxation*, which refers to the decrease of stress over time when it is maintained under constant strain;

https://doi.org/10.4995/YIC2021.2021.13450

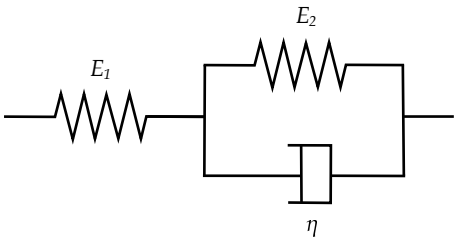

Figure 1: Scheme of the Standard Linear Solid Model with Kelvin-Voigt unit.

3. *Hysteresis*, which describes the dissipation of energy when a material undergoes cyclic loading and unloading.

Similarly, also biological tissues manifest viscoelastic properties. Thus, arteries and veins can be seen, with the due corrections specifically provided by hemodynamics, as highly flexible, viscoelastic tubes, tending almost to collapse under certain physiological conditions in the case of veins, hence leading to deal with highly non-linear systems [16]. Even though frequently, in hemodynamics models, the viscosity of vessels is neglected for simplicity, there is an increasing number of contributions showing the benefits of modeling the mechanical behavior of the vessel wall using a viscoelastic rheological characterization [1].

2 MATHEMATICAL MODELS

2.1 General one-dimensional models

The system of balance laws governing the motion of a compressible fluid through a flexible tube is obtained averaging the 3D compressible Navier-Stokes equations over the cross-section under the assumption of axial symmetry of the geometry of the conduct and of the flow. The resulting 1D non-linear hyperbolic system of partial differential equations (PDEs), composed by the continuity equation and by the momentum equation, reads [17]:

$$\partial_t(A\rho) + \partial_x(A\rho u) = 0 \tag{1a}$$

$$\partial_t(A\rho u) + \partial_x(A\rho u^2 + Ap) - p\,\partial_x A = F_R, \tag{1b}$$

where x is the space, t is the time, A is the cross-sectional area of the tube, ρ is the cross-sectional averaged density of the fluid, u is the averaged fluid velocity, p is the averaged fluid pressure and F_R is a model of the friction between fluid and tube wall, which can either account only for quasi-steady friction effects or both quasi-steady and unsteady ones (for further details the reader can refer to [2]).

Notice that when an incompressible fluid is considered (as for the case of blood flow studies) the system can be written as follows [16]:

$$\partial_t A + \partial_x(Au) = 0 \tag{2a}$$

$$\partial_t(Au) + \partial_x(Au^2) + \frac{A}{\rho}\,\partial_x p = \frac{F_R}{\rho}. \tag{2b}$$

To close system (1), an equation of state (EOS) and a constitutive law (also called *tube law*) must be introduced. In most of the technical applications it is usually sufficient to assume a barotropic behavior of the fluid, therefore $\rho = \rho(p)$. Nevertheless, taking into account cavitation phenomena may be necessary. An EOS for barotropic flows which accounts also for cavitation effects is presented in [10]. On the other hand, to solve system (2), only a proper tube law is needed.

2.2 The augmented fluid-structure interaction systems

The tube law describes the relationship between the tube cross-section and the internal pressure, containing all the information about the mechanical behavior of the pipe material. To correctly model the compliance and the flexibility of plastic ducts, in this work the Standard Linear Solid (SLS) model is considered, being the simplest viscoelastic rheological model able to describe the three main features of viscoelastic materials [14]. Hence, we assume that the mechanical behavior of the wall is defined by the interaction of a linear spring in series with a Kelvin-Voigt unit, composed of a linear spring in parallel with a linear dash-pot, as presented in Figure 1.

Evaluating the constitutive equation of the SLS model, expressed in terms of stress σ and strain ϵ,

$$\mathrm{d}_t\sigma = E_0\,\mathrm{d}_t\epsilon - \frac{1}{\tau_r}(\sigma - E_\infty\epsilon), \tag{3}$$

the three parameters of the model, namely the instantaneous Young modulus E_0, the asymptotic Young modulus E_∞, and the relaxation time τ_r, are so defined (referring to Figure 1):

$$E_0 = E_1, \qquad E_\infty = \frac{E_1E_2}{E_1+E_2}, \qquad \tau_r = \frac{\eta}{E_1+E_2}. \tag{4}$$

From equation (3), concerning a compressible fluid and a mildly non-linear system (1), applying Barlow's formula, introducing the linearized kinematic relation between the strain and the non-dimensional cross-sectional area rescaled with respect to its reference value $\alpha = \frac{A}{A_0} = (1+\epsilon^2) \approx 1+2\epsilon$, and recurring to the continuity equation (1a), the following PDE form of the SLS rheological law is obtained [2, 13]:

$$\partial_t A + d_1\,\partial_x(A\rho u) = S_1, \tag{5}$$

where

$$d_1 = \frac{2c_s^2}{2\rho c_s^2 + K\alpha}, \qquad S_1 = \frac{1}{\tau_r}\left[\frac{2A}{2\rho c_s^2 + K\alpha}(p-p_0) - \frac{E_\infty}{E_0}\frac{AK}{2\rho c_s^2 + K\alpha}(\alpha-1)\right].$$

Here, K represents the stiffness of the material, which accounts for the instantaneous Young modulus E_0, the wall thickness and the radius of the tube, $c_s = \sqrt{\frac{\partial p}{\partial \rho}}$ is the celerity contribute related to the compressibility of the fluid, which results equal to the sound speed when cavitation does not occur [2], and p_0 is the equilibrium pressure.

It can be observed that the relaxation time τ_r, and therefore the viscosity coefficient η, affects only the source term S_1. In fact, the viscous information about the FSI mechanism are all embedded in the term S_1, which defines viscoelastic damping effects. Interestingly, if we let $\tau_r \to 0$, entering in the diffusive and stiff regime of the system, from equation (3) we recover exactly the Laplace law, which is the standard elastic law used in literature [13]. Therefore, the hyperbolic augmented fluid-structure interaction (a-FSI) system for compressible fluids and mildly non-linear systems, capable of describing from simple elastic to viscoelastic FSI mechanisms, results

$$\partial_t(A\rho) + \partial_x(A\rho u) = 0 \tag{6a}$$
$$\partial_t(A\rho u) + \partial_x(A\rho u^2 + Ap) - p\,\partial_x A = F_R \tag{6b}$$
$$\partial_t A + d_1\,\partial_x(A\rho u) = S_1. \tag{6c}$$

Notice that to allow a formally correct treatment of possible discontinuous longitudinal changes of the reference cross-section or of the mechanical parameters of the wall, it is possible

to account for trivial equations which simply states that the interested variables are constant in time [2, 3].

A similar procedure can be followed also when considering blood flow models, hence an incompressible fluid and a highly non-linear setting, as in system (2), which leads to analogous results. Indeed, defining $\epsilon = \alpha^m - \alpha^n$, where parameters m and n are associated to the specific behavior of the vessel wall, whether arterial or venous [15], and using this definition in equation (3) together with Barlow's formula, recurring also to the continuity equation (2a), the following PDE of the SLS model is obtained [3, 4]:

$$\partial_t p + d_2\, \partial_x(Au) = S_2, \tag{7}$$

with

$$d_2 = \frac{K}{A}\left(m\alpha^m - n\alpha^n\right), \qquad S_2 = \frac{1}{\tau_r}\left[\frac{E_\infty}{E_0} K\left(\alpha^m - \alpha^n\right) - (p - p_0)\right].$$

The reader is invited to observe the similarities between d_1, S_1 and d_2, S_2. In particular, also in this configuration, the source term S_2 accounts for all the viscoelastic information of the FSI mechanism, and if we consider the diffusive limit letting $\tau_r \to 0$, we recover again the corresponding elastic tube law [3, 5]. Hence, the final hyperbolic a-FSI system for blood flow results:

$$\partial_t A + \partial_x(Au) = 0 \tag{8a}$$

$$\partial_t(Au) + \partial_x(Au^2) + \frac{A}{\rho}\partial_x p = \frac{F_R}{\rho} \tag{8b}$$

$$\partial_t p + d_2\, \partial_x(Au) = S_2 \tag{8c}$$

It is worth to underline that the choice of inserting the tube law in PDE form straight inside the system of equations results advantageous if compared to approaches generally followed in literature [1, 15]. Indeed, if the classical formulation is adopted choosing to characterize the FSI with the Kelvin-Voigt viscoelastic model (which, anyhow, lacks in the description of the relaxation process of the stress [14]), a second order derivative in space of the flow rate Au arises, which leads to deal with a non-hyperbolic system and consequent numerical issues.

Finally, to obtain more flexible models, it is possible to extend the number of Kelvin-Voigt units in the SLS configuration, obtaining the so-called Kelvin-Voigt chain [14]. Theoretically, the more elements we have, the more accurate our model will be in describing the real response of the material. Conversely, the more complex the model is, the more parameters that must be calibrated there are. The extension for the case of water pipelines is presented in details in [2].

3 NUMERICAL METHODS

Initially, to solve system (6), three different numerical schemes have been chosen and compared: the widely used Method of Characteristics (MOC) [7], an explicit path-conservative finite volume (FV) method associated with the Dumbser-Osher-Toro (DOT) Riemann solver [9], and a semi-implicit (SI) FV method specifically developed for axially symmetric compressible flows in compliant tubes [10].

On the other hand, to solve system (8), which can result *stiff* under physiological conditions, an Implicit-Explicit (IMEX) Runge-Kutta scheme, proposed for applications to hyperbolic systems with stiff relaxation terms, is considered [18]; while, for the space discretization, the same FV method with DOT solver previously mentioned is used. In particular, the second-order IMEX-SSP2(3,3,2) scheme is adopted [18]. The chosen numerical scheme is asymptotic preserving (AP) and asymptotic accurate in the zero-relaxation limit (i.e. when $\tau_r \to 0$), which

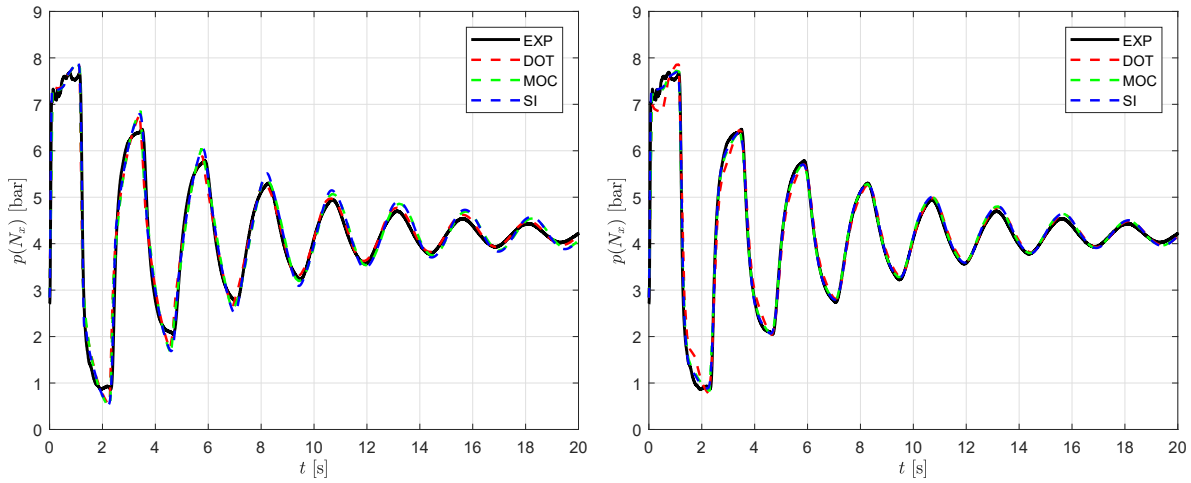

Figure 2: Comparison of the numerical results obtained with MOC, DOT and SI schemes against the experimental solution (EXP) of the water hammer test when using the SLS model (left) or the Kelvin-Voigt chain (right). Pressure $p(N_x)$ at the downstream end.

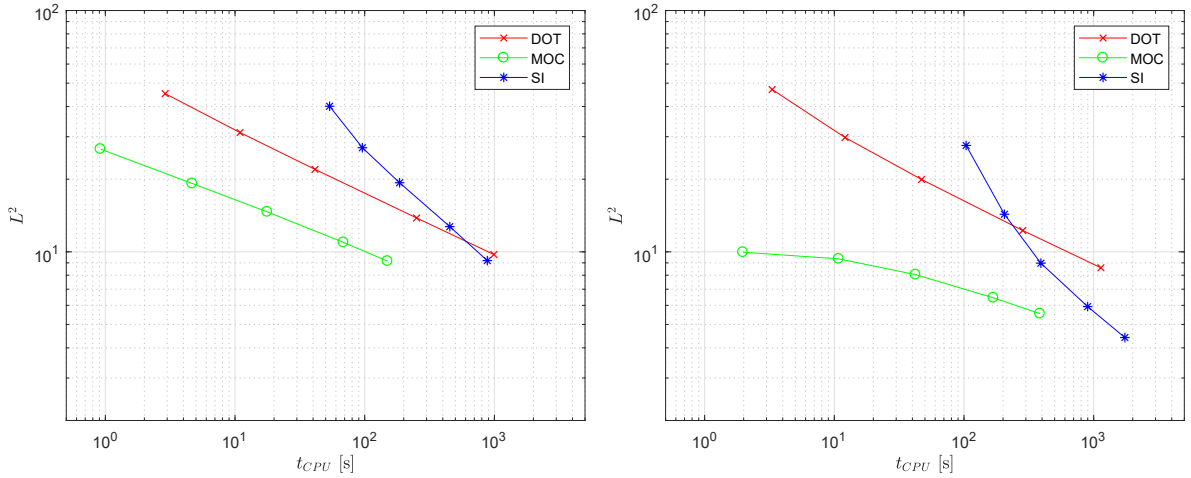

Figure 3: Results of the efficiency analysis for the water hammer test with the SLS model (left) and Kelvin-Voigt chain (right), in terms of L^2 norm with respect to the CPU time t_{CPU}.

allows to preserve the consistency of the scheme in the equilibrium, elastic limit as well as the order of accuracy, without restrictions due to the scaling parameters [5]. Another advantage of the chosen scheme lays in the possibility to analytically linearize each Runge-Kutta step to obtain a totally explicit algorithm, avoiding the adoption of iterative procedures like Newton-Raphson method, with a consequent consistent reduction of the computational cost [3].

4 NUMERICAL RESULTS AND DISCUSSION

To validate the proposed methodologies, different numerical tests have been designed. To compare the numerical methods used to solve system (6), a water hammer test case is here presented, with reference experimental data taken from [12], for which both the SLS model and the Kelvin-Voigt chain with 5 units are used.

Concerning the a-FSI blood flow model (8), targeted comparisons between numerical results and literature benchmarks have been performed with respect to close to reality test cases in single portions of vessels. In addition, patient-specific tests are considered, for which it has been possible to compare numerical results with available pressure data recorded in-vivo, from

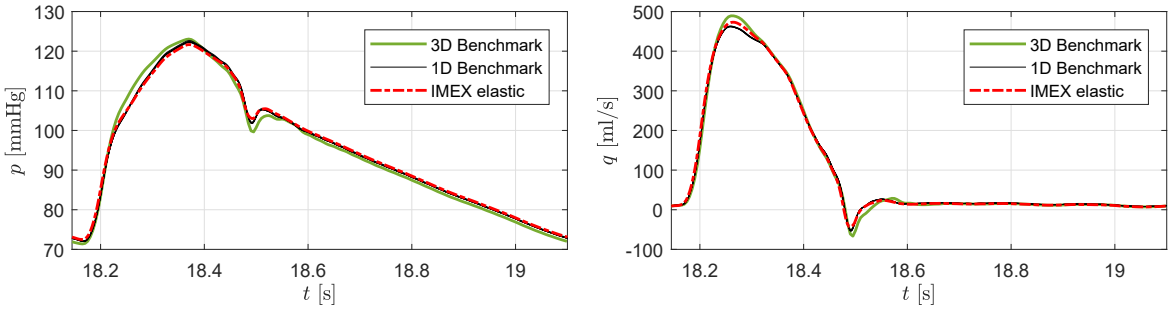

Figure 4: Baseline upper thoracic aorta case. Results obtained solving the 1D a-FSI system with the IMEX FV scheme with elastic tube law compared to six 1D and one 3D benchmark solutions. Results presented in terms of pressure at the midpoint (left) and flow rate at the midpoint (right).

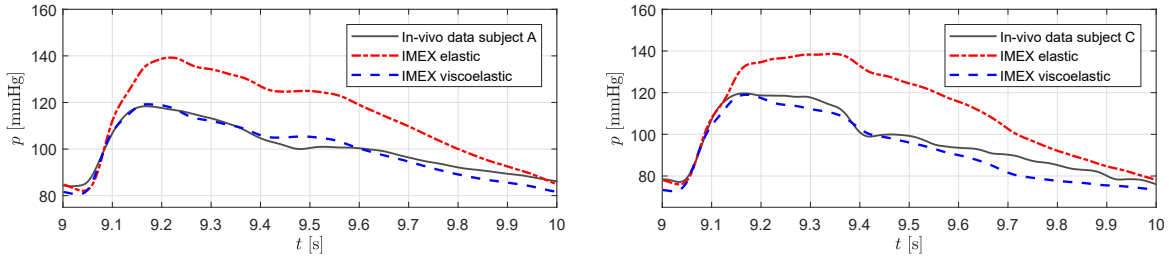

Figure 5: Patient-specific common carotid artery cases. Results obtained solving the 1D a-FSI system with the IMEX FV scheme, with elastic and viscoelastic tube law, for a 29 years old subject (left) and a 44 years old subject (right), in terms of pressure, compared with measured data.

different volunteers' common carotid arteries [4].

4.1 Water hammer tests

Following [12], a DN50 (22.0 mm radius) high-density polyethylene (HDPE) pipe is considered, with length 203.3 m and a flow rate of 2.0 l/s. In order to experimentally generate the transient wave, a closure maneuver was performed to a valve positioned downstream of the pipeline, with a closure time of 0.1 s. For this test, viscoelastic parameters have been calibrated using the SCE-UA (Shuffled Complex Evolution - University of Arizona) algorithm [8]. From Figure 2, it can be verified that the three numerical methods reproduce similar results, both using the SLS model or the extended Kelvin-Voigt chain. At the same time, it is observed that the increment of viscoelastic parameters does not return a consistent increase in the quality of the final result, weighing, on the other hand, in terms of computational cost and difficulty of calibration of the parameters. In fact, for the same water hammer test, an efficiency analysis has been computed to evaluate the performance of each numerical scheme adopted. Observing results shown in Figure 3, it is visible that the increment of viscoelastic parameters to characterize the material mechanics leads to an inevitable increment of computational costs not balanced by a comparable error reduction.

4.2 Blood flow tests

A baseline upper thoracic aorta test case is simulated, following [6], using a purely elastic wall model to allow comparisons with benchmark data available in literature. Figure 4 shows a comparison of the numerical results obtained solving the a-FSI system with the IMEX FV scheme with respect to six 1D and one 3D benchmarks [6]. It can be noticed that, for both pressure and flow rate, IMEX results are in perfect agreement with benchmarks.

Because no reference solutions of blood flow simulations on single vessels assuming a vis-

coelastic FSI are available in literature, flow velocity and pressure data measured in-vivo from four common carotids and two femoral arteries of volunteer subjects have been used to set up patient-specific test cases, to validate the proposed model in its viscoelastic configuration. The velocity wave extrapolated from each of the six subjects, obtained by Doppler measurements, is prescribed as inlet condition, while the post-processed pressure wave, measured recurring to the Arterial Tonometry technique, is used for comparisons with numerical results [4]. These simulations have been performed using both the elastic model and the viscoelastic law, to evaluate the effects of viscoelasticity in arterial hemodynamics. Viscoelastic parameters have been calibrated following [4]. Results of the test cases obtained for two patient-specific common carotid arteries are here reported in Figure 5, from which the excellent agreement between in-vivo measured and numerical pressure wave, obtained with the proposed methodology, can be observed. Indeed, these results confirm the capability of the proposed model to reproduce realistic pressure signals and the importance of taking into account the viscosity of the vessel wall in order not to overestimate systolic pressure values.

REFERENCES

[1] Alastruey, J., Khir, A. W., Matthys, K. S., Segers, P., Sherwin, S. J., Verdonck, P. R., Parker, K. H., Peiró, J. Pulse wave propagation in a model human arterial network: Assessment of 1-D visco-elastic simulations against in vitro measurements. *J. Biomech.*, 44(12):2250–2258 (2011).

[2] Bertaglia, G., Ioriatti, M., Valiani, A., Dumbser, M., Caleffi, V. Numerical methods for hydraulic transients in visco-elastic pipes. *J. Fluids Struct.*, 81:230–254 (2018).

[3] Bertaglia, G., Caleffi, V., Valiani, A. Modeling blood flow in viscoelastic vessels: the 1D augmented fluid–structure interaction system. *Comput. Methods Appl. Mech. Eng.*, 360(C):112772 (2020).

[4] Bertaglia, G., Navas-Montilla, A., Valiani, A., Monge García, M. I., Murillo, J., Caleffi, V. Computational hemodynamics in arteries with the one-dimensional augmented fluid-structure interaction system: viscoelastic parameters estimation and comparison with in-vivo data. *J. Biomech.*, 100(C):109595 (2020).

[5] Bertaglia, G., Caleffi, V., Pareschi, L., Valiani, A. Uncertainty quantification of viscoelastic parameters in arterial hemodynamics with the a-FSI blood flow model. *J. Comput. Phys.*, 430:110102 (2021).

[6] Boileau, E., Nithiarasu, P., Blanco, P. J., Müller, L. O., Fossan, F. E., Hellevik, L. R., Donders, W. P., Huberts, W., Willemet, M., Alastruey, J. A benchmark study of numerical schemes for one-dimensional arterial blood flow modelling. *Int. J. Numer. Method. Biomed. Eng.*, e02732:1–33 (2015).

[7] Covas, D. I. C., Stoianov, I., Mano, J. F., Ramos, H., Graham, N., Maksimovic, C. The dynamic effect of pipe-wall viscoelasticity in hydraulic transients. Part II - model development, calibration and verification. *J. Hydraul. Res.*, 43(1):56–70 (2005).

[8] Duan, Q. Y., Gupta, V. K., Sorooshian, S. Shuffled complex evolution approach for effective and efficient global minimization. *J. Optim. Theory Appl.*, 76(3):501–521 (1993).

[9] Dumbser, M., Toro, E. F. A simple extension of the Osher Riemann solver to non-conservative hyperbolic systems. *J. Sci. Comput.*, 48:70–88 (2011).

[10] Dumbser, M., Iben, U., Ioriatti, M. An efficient semi-implicit finite volume method for axially symmetric compressible flows in compliant tubes. *Appl. Numer. Math.*, 89:24–44 (2015).

[11] Ferras, D., Manso, P., Schleiss, A., Covas, D. One-Dimensional Fluid–Structure Interaction Models in Pressurized Fluid-Filled Pipes: A Review. *Appl. Sci.*, 8(10):1844 (2018).

[12] Evangelista, S., Leopardi, A., Pignatelli, R., de Marinis, G. Hydraulic Transients in Viscoelastic Branched Pipelines. *J. Hydraul. Eng.*, 141(8):04015016 (2015).

[13] Leibinger, J., Dumbser, M., Iben, U., Wayand, I. A path-conservative Osher-type scheme for axially symmetric compressible flows in flexible visco-elastic tubes. *Appl. Numer. Math.*, 105:47–63 (2016).

[14] Lakes, R. Viscoelastic Materials. *Cambridge University Press* (2009).

[15] Montecinos, G. I., Müller, L. O., Toro, E. F. Hyperbolic reformulation of a 1D viscoelastic blood flow model and ADER finite volume schemes. *J. Comput. Phys.*, 266:101–123 (2014).

[16] Formaggia, L., Quarteroni, A., Veneziani, A. *Cardiovascular Mathematics: Modeling and simulation of the circulatory system.* Springer (2009).

[17] Ghidaoui, M. S., Zhao, M., McInnis, D. A., Axworthy, D. H. A Review of Water Hammer Theory and Practice. *Appl. Mech. Rev.*, 58(1):49–76 (2005).

[18] Pareschi, L., Russo, G. Implicit-explicit Runge-Kutta schemes and applications to hyperbolic systems with relaxation. *J. Sci. Comput.*, 25:129–155 (2005).

[19] Shaw, M. T., MacKnight, W. J. *Introduction to Polymer Viscoelasticity: Third Edition.* John Wiley & Sons, Inc. (2005).